Carbohydrate Polymers **21** (1993) 39–46

Distribution of uronate residues in alginate chains in relation to alginate gelling properties — 2: Enrichment of β-D-mannuronic acid and depletion of α-L-guluronic acid in sol fraction

Bjørn T. Stokke,[a] Olav Smidsrød,[b] Flavio Zanetti,[c] Wenche Strand[b] & Gudmund Skjåk-Bræk[b]

[a]*Department of Physics,* [b]*Department of Biotechnology, Norwegian Biopolymer Laboratory, University of Trondheim, NTH, N-7034 Trondheim, Norway*

[c]*POLY-bios Research Centre, LBT — Area di Ricerca, Padriciano 99, I-34012 Trieste, Italy*

(Received 4 November 1992; accepted 3 December 1992)

Alginate, a copolymer comprised of β-D-mannuronic and α-L-guluronic acid isolated from seaweeds and extruded by certain bacteria, forms a gel in combination with several divalent cations. Polymer chains leaching out at 7°C, 24°C and 50°C from Ca-, and Sr-alginate gel beads were found to be depleted in α-L-guluronic acid and enriched in β-D-mannuronic acid compared to the starting material. For Sr gels, leached material is found to be almost devoid of α-L-guluronic acid triplets for the Sr gels, and a significant reduction in such triplets compared to the starting material was observed for the polymers leached from the Ca-gels. The leached material was also found to comprise the low-molecular-weight tail of the starting material molecular weight distribution, the truncation towards lower molecular weight was larger for the more block-like alginate. The chemical composition of the leaching out from Sr-gels and Ca-gels suggests that 3 and 8 ± 2 contiguous α-L-guluronic acid residues are required to form stable junction zones for Sr- and Ca-induced gelation respectively.

INTRODUCTION

Alginates are statistical copolymers of (1 → 4) linked residues of β-D-Man*p*A (M) and α-L-Gul*p*A (G) acid. The average composition and sequential arrangement of the two uronic acids depends on the seaweed from which they are isolated. This family of polysaccharides are widely used in various processes and products due to their ability to form highly viscous solutions, or gels by complexing with divalent metal ions, e.g. Ca^{2+} or Sr^{2+}. The mild gelling conditions of Ca^{2+}-complexed alginate compared to other polymeric gels has also lead to extensive use in biotechnology and biomedicine to immobilise or encapsulate enzymes and living cells (Smidsrød & Skjåk-Bræk, 1990). The potential of this technique has recently been shown by the use of implanted alginate immobilized Langerhans islets to reverse diabetes mellitus on spontaneous diabetic dogs up to 8 months (Soon-Shiong *et al.*, 1992).

In a previous paper (Stokke *et al.*, 1991), the authors considered explicitly the effect of the number of consecutive α-L-Gul*p*A residues on the dimerisation occurring upon formation of a junction zone in the egg-box model for alginate gelation (Grant *et al.*, 1973; Thom *et al.*, 1982). Analysis of the pairwise interaction of oligoguloronate indicated that there is a transition from unpaired to paired oligoguloronate residues as the degree of polymerisation increases. This cooperative transition was subsequently approximated by a step function between the paired and unpaired G-sequences occurring at a critical degree of polymerisation, LG_{min}. The parameter LG_{min} was expected to depend on polymer concentration, type of ion used for crosslinking alginate as well as the actual temperature. The model was tested against previous published experimental data and semi-quantitative agreement between model predictions and experimental data were reported. The aim of this study is to extend the experimental testing of

Carbohydrate Polymers 0144-8617/93/$06.00

the theoretical description by determining the amount of, the molecular weight distribution and the chemical composition of the material leaching out from alginate gel beads. This was carried out using alginates of different chemical compositions and sequences obtained from various sources. The material leaching out from the alginate gels, the sol fraction, is assumed not to contain any G-blocks of length LG_{min} or larger. The experiments were designed not only to test this gelation model, but because the material leaching out from the alginate gel beads may have a different affect on the immune system compared with the initial material. Thus, these results also have practical relevance from the point of view of biomedical applications.

EXPERIMENTAL

Materials

Sodium alginate with a high content of transition frequencies was prepared from old tissue of *Ascophyllum nodosum*. Alginate rich in guluronic acid, *Laminaria hyperborea* stipe (samples PT 28 and PT180), was obtained from Protan Biopolymer A/S (Drammen, Norway). A sample prepared from *Macrocystis pyrifera* was obtained from the Kelco Division of Merck, (San Diego, CA, USA). The commercial alginates were purified by dissolution in 0·2% aqueous sodium chloride, followed by precipitation with ethanol and washing with ethanol and ether before drying.

Experimental procedures

Nuclear magnetic resonance (NMR) spectroscopy
The proton spectra were recorded at 92°C using a Bruker WM-500 or a Jeol FX-100 spectrometer. The latter spectrometer was also used to obtain the 25 MHz ^{13}C NMR spectra. The monomer composition, diad and G-centred triad frequencies were determined from the ^{1}H-spectra as described previously (Grasdalen, 1983), and the M-centred triads were obtained from the ^{13}C-spectra (Grasdalen *et al.*, 1981). These compositional data are given in Table 1.

Leaching of alginate from alginate gels (preparative)
The gel beads were prepared by allowing droplets of aqueous sodium alginate (200 ml, 2% w/v) to fall into an aqueous solution of 0·1 M $CaCl_2$ or 0·1 M $SrCl_2$. The viscous solution was pressed through a syringe (1·0 mm) and the size of the droplets was controlled by applying a coaxial airstream (Martinsen *et al.*, 1989). The gel beads were then kept in the calcium chloride, or strontium chloride solution for 24 h. They were 2 mm in diameter and had a final polymer concentration after correction for shrinkage of 2·6–3·4% w/v. The beads were washed with distilled water and suspended in 500 ml saline (0·9% NaCl). These suspensions of the gel beads were kept at 7°C, 24°C and 50°C on a gyratory shaker and the sodium chloride solution was changed every 4 days. The sodium chloride solutions were pooled, concentrated by evaporation, and dialyzed against 0·05 M triethylenetetraminehexa-acetic acid (TTHA), pH 7·0 for 24 h and exhaustively against water. The soluble polymeric material was collected by freeze-drying.

Leaching of alginate (analytical)
Ca-, and Sr-alginate beads were formed as described above from 10 ml of 1·5% sodium alginate. After gelling had been completed the beads were suspended in 100 ml saline (0·9% NaCl). The leached material was analysed as the total soluble carbohydrate by the phenolic sulphuric colour reaction according to Dubois *et al.* (1956).

Gel permeation chromatography – low angle laser light scattering (GPC–LALLS)
Molecular weight distributions were obtained using analytical GPC equipped with an on-line LALLS detector. The system consisted of an injector (Rheodyne 7125), a pump (Jasco BIP/1), a LALLS detector (LDC-Chromatix CMX-100 equipped with a He–Ne laser, λ_0 = 632·8 nm) and a concentration-sensitive detector (refractive index (RI) Waters Mod. 410). Two serially connected GPC columns TSK G 5000 PW and TSK G 6000 PW (LKB Bromma, Sweden) with guard column TSK PWH were used. The RI and the LALLS signals for each point of the chromatogram were analysed by a IBM-XT-based software (Chromatix PC-LALLS™), corrected for delay and instrumental parameters. This provided both the differential and the cumulative molecular distribution curves for the given sample. The RI signal was also sent to a Digital P350 via an acquisition system Waters SIM, to be processed by means of the Waters 840 software for relative GPC determination. In this way comparison between absolute (i.e. LALLS) and relative molecular weight

Table 1. Alginate sources and chemical composition

Source	F_G	F_M	F_{GG}	F_{GM}	F_{MM}	F_{GGG}	F_{GGM}	F_{MGM}	$L_{G>1}$
A. nodosum	0·43	0·57	0·20	0·23	0·34	0·12	0·08	0·15	3·5
M. pyrifera	0·42	0·58	0·22	0·20	0·38	0·17	0·05	0·15	5·4
L. hyperborea	0·68	0·32	0·56	0·12	0·20	0·51	0·05	0·07	12·2

distribution determination methods was achieved on the same chromatographic run (Martinsen *et al.*, 1991). The solutions were filtered through a Millipore 0·22 μm filter prior to all LALLS experiments. The injected sample volume was 20 μl. The polymer concentration ranged from 0·5 to 2 g litre^{-1}.

RESULTS

The experimentally determined sol fraction for alginate from five sources were found to depend on average G-block length $L_{G>1}$, the gel-complexing ion and the molecular weight distribution within the samples. The amount of alginate leaking out from alginate gel beads were found to be of the order of 1–4% of the starting material (Fig. 1). Leaching was almost complete within 2 weeks at room temperature, which agrees with the previously reported experiments (Stokke *et al.*, 1991). Exchanging Ca^{2+} with Sr^{2+} yielded a decrease in the sol fraction of alginate leaching from *Laminaria hyperborea* PT180 (Fig. 1). It has previously been reported (Stokke *et al.*, 1991) that decreasing the average G-block length increases the experimentally determined sol fraction when using the same ion and comparable molecular weight distributions. The amount of material leached is also expected to depend on the molecular weight distribution of the sample.

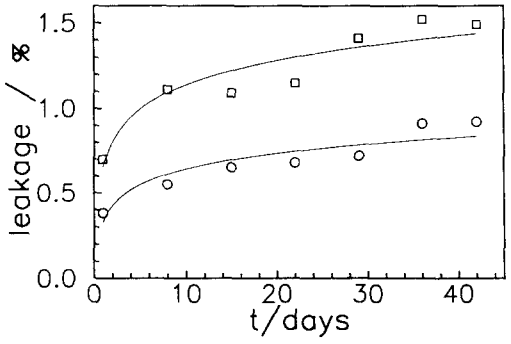

Fig. 1. Fraction (%) of alginate leaching out of (□) Ca-alginate, and (○) Sr-alginate gel beads of alginate from *L. hyperborea* PT 180 versus time.

Figure 2 shows the molecular weight distribution of the initial material and the sol fraction of Ca^{2+} alginate gel beads for alginate from *Ascophyllum nodosum* having $L_{G>1}$ = 3·5, *Macrocystis pyrifera* having $L_{G>1}$ = 5·4, *L. hyperborea* having $L_{G>1}$ = 12·2. The sol fraction comprises the low-molecular-weight tail of the initial molecular weight distribution for these four alginate samples. The total amount leaching out from the alginate gel beads depends on fraction of material that can leach out in the initial distribution. This means that comparison of the amounts leaching out from different alginate samples does not provide insight into the underlying molecular mechanism unless the molecular weight distributions are known. Figure 3 shows the accumulated weight fraction versus molecular weight for the experimentally determined sol fraction of the Ca-gels. These data indicate that the highest molecular weight present in the sol fraction is decreasing with increasing $L_{G>1}$. This could be seen despite uncertainty in the determination of the low-molecular-weight tail because of limited column resolution and the non-linear calibration in the low-molecular-weight tail of the samples.

The ^{1}H NMR spectra of the original alginate samples and the material leaching from Ca-gel and Sr-gel beads showed that the amount of triplets of α-L-Gul*p*A was greatly diminished in the experimentally determined sol fraction compared to the starting material. The

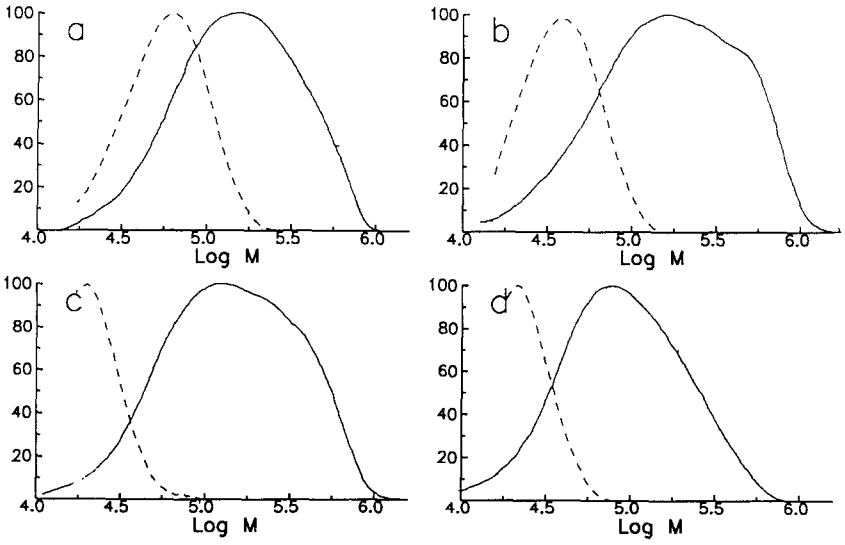

Fig. 2. Molecular weight distributions of ( ) original alginate samples and ( ) alginate leaching from Ca-gel beads of alginate from (a) *A. nodosum*, (b) *M. pyrifera* medium η, (c) *L. hyperborea* PT 180 and (d) *L. hyperborea* PT 28.

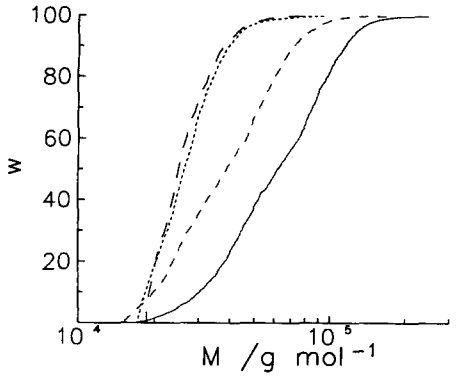

Fig. 3. Cumulated molecular weight distributions of alginate leaching from Ca-gel beads of alginate from (———) *A. nodosum*, (– – –) *M. pyrifera* medium η, (------) *L. hyperborea* PT 180, and (— —) *L. hyperborea* PT 28.

depletion in GGG triplets is larger for the material leaching from Sr-gel beads compared with Ca-gel beads. Tables 2 and 3 summarise the chemical composition of the material leaching from Ca-gels and Sr-gels, respectively. These data shows that the chemical composition of the leached material differs from that of the source material and depends on the ion used to induce the gel-formation. The general trends are that the leached materials are enriched in both M content and MM-doublets, and depleted in G content, doublets and triplets. These changes are more pronounced in the material leaching from the Sr-gels compared with the Ca-gels. The differences among the material leaching from the various alginate sources are less than within the starting material (Tables 1-3). Because the NMR data indicate that these non-functional chains leaching out are depleted in oligoguluronate sequences, these changes are largest for the starting material having the largest fraction of long G-blocks, i.e. for alginates isolated from *L. hyperborea*.

The data on chemical composition of the sol fraction of Ca-gels and Sr-gels of *L. hyperborea* at 7 and 50°C were essential identical to the data obtained at 24°C.

DISCUSSION

The experimentally determined data presented here allows testing of the previously developed theoretical model in three different ways. First, the existence of a LG_{min} independent on the alginate source but depending on the complexing ion can be tested by considering the residue sequence of the material leaching out from the gel beads. Secondly, the high-molecular-weight cutoff of the molecular weight distribution in the experimentally determined sol fraction can be compared with that predicted. Thirdly, the experimentally determined changes in the chemical composition and sequence of the sol fraction relative to that of the starting material can be compared to those predicted using the experimentally established LG_{min}.

It is assumed in the following that the changes in chemical composition, molecular weight distribution and amount of material leaching out of the alginate beads arises solely from chains that are not able to bind to the gel network in view of the gelation model developed previously. This implies that the experimentally determined sol fraction can not contain any sequences of G-residues equal to or larger than the critical length LG_{min}. The previous finding (Martinsen *et al.*, 1991) that there are only smaller differences in chemical composition and sequence information within fractions of alginate from *Laminaria hyperborea* and *Macrocystis pyrifera* separated preparatively on a Sepharose Cl-6B–Sepharose CL-4B set-up exclude the possibility that the present observations of changes in chemical composition of the sol fraction arises as a

Table 2. Chemical composition of alginate leaching from Ca-alginate gels (T = 24°C)

Source	F_G	F_M	F_{GG}	F_{GM}	F_{MM}	F_{GGG}	F_{GGM}	F_{MGM}	$L_{G>1}$
A. nodosum	0·28	0·72	0·14	0·14	0·58	0·07	0·07	0·07	3·0
M. pyrifera low η	0·22	0·78	0·07	0·15	0·63	0·03	0·04	0·12	2·9
M. pyrifera medium η	0·19	0·81	0·08	0·11	0·70	0·05	0·03	0·07	3·5
L. hyperborea PT 180	0·32	0·68	0·23	0·09	0·59	0·16	0·07	0·02	4·4
L. hyperborea PT 28	0·23	0·77	0·12	0·11	0·66	0·08	0·04	0·06	3·7

Table 3. Chemical composition of alginate leaching from Sr-alginate gels (T = 24°C)

Source	F_G	F_M	F_{GG}	F_{GM}	F_{MM}	F_{GGG}	F_{GGM}	F_{MGM}	$L_{G>1}$
A. nodosum	0·16	0·84	0·06	0·10	0·74	0·00	0·06	0·04	2·0
M. pyrifera low η	0·12	0·88	0·04	0·08	0·80	0·00	0·04	0·04	2·0
M. pyrifera medium η	0·12	0·88	0·03	0·09	0·79	0·00	0·03	0·05	2·0
L. hyperborea PT 180	0·09	0·91	0·03	0·06	0·84	0·00	0·03	0·03	2·0
L. hyperborea PT 28	0·09	0·91	0·03	0·06	0·85	0·00	0·03	0·03	2·0

consequence of the shift in molecular weight. Analyses of the sequence information of the experimentally determined sol fraction may therefore establish LG_{min}.

The NMR data of the material leaching from the Sr-gel beads indicate that the longest sequences of G in the sol fraction are 2 (Table 3). This same truncation of the G-block distribution in the material leaching out is found for all the five samples from the three different sources included in this study. This means that one Sr^{2+} coordinated to two pairs of GG blocks is not sufficient to form a junction zone. This should consequently yield $LG_{min}(Sr^{2+}) = 4$ since even numbers of LG_{min} are expected to represent the most stable states (Stokke *et al.*, 1991). The experimental finding that the F_{GGG} for the Sr^{2+} leaching are practically absent (Table 3) suggest that $LG_{min} = 3$. Ion complexation of two GGG trimers in register would represent one fully and one partly coordinated ion with a difference in interaction energy (Fig. 4(A)). The out-of-register zipper for equally long G-sequences at $LG_{min} = 3$ (Fig. 4(B)) would yield less interaction energy in the junction zones and is therefore not considered to be an efficient association mode. On the other hand, the heterogeneous duplex (Fig. 4(C)) is expected to represent a viable junction zone. Note that in the present discussion of the chemical composition of the sol fraction, there is no requirement that all junction zones are made up of homogeneous duplexes.

Determination of parameter $LG_{min}(Ca^{2+})$ is not as straightforward as for Sr^{2+} because that there is no clear truncation within the length of the G-blocks directly observable by NMR. The second order Markov chain were therefore applied to the data on the sol fraction analogously as done previously for the whole sample (Stokke *et al.*, 1991) in trying to gain some information about the parameter $LG_{min}(Ca^{2+})$. Using the same procedure as in the previous model sol fraction (Stokke *et al.*, 1991), it is clear that this approach does not reproduce the distribution of the G-blocks, but on the other hand, other sequence models of the sol fraction of Ca-alginate gels would require additional parameters. It should be noted that the second order Markov model accurately reproduce the G-block distribution of the sol fraction of the Sr-alginate gels since the truncation of the G-block distribution occurs within the experimentally accessible sequence information. The calculated G-block distribution in the experimentally determined sol fraction of the Ca-gels are clearly shifted towards longer G-blocks compared to that of the Sr-gels (Figs 5(A) and 5(B)). At the same time there are less source-dependence than in the original material, but smaller variations remains. These calculated G-block distributions show a truncation in the range $LG_{min} = 6$–10 for the material leaching from the Ca gels (Fig. 5(B). Because of the limited validity of this calculation, the estimate $LG_{min}(Ca^{2+}) = 8 \pm 2$ will be used in the further testing of the model predictions.

The average block length of the G-blocks larger than one residue, $L_{G>1}$, also shows a shift from the source-dependent values for the starting material (Table 1), to the source independent, but ion-dependent values for the material leaching out from the Ca-gels (Table 2) and Sr-gels (Table 3). The averages within the samples are $L_{G>1} = 3{\cdot}5$ and $2{\cdot}0$ for the sol fractions of the Ca-gels and Sr-gels, respectively. The parameters LG_{min} and $L_{G>1}$ represent the cutoff and an average within the G-blcok distribution, and the correlation between them is expected to reflect the actual distribution. Note that since both these parameters for the sol fractions are independent of the source and depend on the gel inducing ion, the requirement of a G-block sequence to exceed a lower critical length in being able to form a stable junction zone, is strongly suggested.

The above finding that $LG_{min}(Ca^{2+})$ and $LG_{min}(Sr^{2+})$ are practically independent of the source and $LG_{min}(Ca^{2+}) > LG_{min}(Sr^{2+})$ are in agreement with the earlier predictions (Stokke *et al.*, 1991). The difference in LG_{min} for the Ca^{2+} and the Sr^{2+} ion can also be considered in view of the experimentally determined selectivity coefficient $K^{Sr}_{Ca} = 7$ (Haug & Smidsrød, 1970). From an energetic point of view, this selectivity

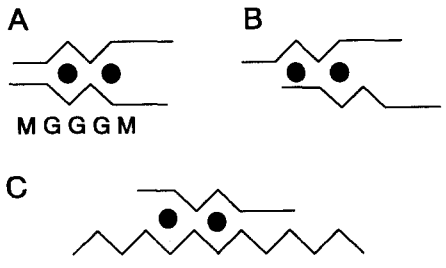

Fig. 4. Schematic graphical representation of association modes of G-sequences at length $LG_{min} = 3$ depicting (A) perfectly matched, (B) mismatched, and (C) G-sequence length heterogeneity. The α-L-Gul*p*A (G) and β-D-Man*p*A (M) residues are represented as zig-zags and horizontal lines, respectively. The $LG_{min} = 3$ is selected according to the value found for Sr^{2+}-induced gelation.

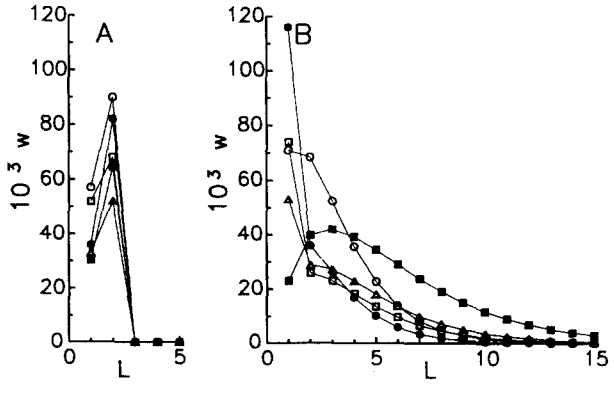

Fig. 5. Calculated G-block distribution in experimentally determined sol fraction of (A) Sr- and (B) Ca-gels. The alginate sources are (●) *A. nodosum*, (□) *M. pyrifera* low η, (○) *M. pyrifera* med η, (△) *L. hyperborea* PT 180, and (■) *L. hyperborea* PT 28.

corresponds to a free energy difference of $RT \ln 7 = 4{\cdot}7$ kJ mol^{-1} (ion) at room temperature. Assuming that the energy gain in the Ca- and Sr-complexed homogenous G-block duplex of length LG_{min} is identical, the energy gain is calculated to 2·9 kJ mol^{-1} and 7·6 kJ mol^{-1} for Ca- and Sr-complexation, respectively. Parameters $LG_{min}(Ca^{2+}) = 8$ and $LG_{min}(Sr^{2+}) = 3$ were used in this calculation. The value for Ca-complexation thus obtained is about the same as the 3 kJ mol^{-1} reported by Cesaro *et al.* (1982). The observed small shift in chemical composition of the sol fraction at 7 and 50°C indicate that LG_{min} are less affected by such a temperature shift than by exchange of ions.

The upper limit of the molecular weight distribution in the experimentally determined sol fraction from Ca-alginate gels is inversely related to $L_{G>1}$. The 90% percentiles in the accumulated molecular weight distribution covers almost a factor of three, with $M_{90\%}(L_{G>1} = 3{\cdot}5) = 115 \times 10^3$ g mol^{-1} (*Ascophyllum nodosum*) being the largest and $M_{90\%}(L_{G>1} = 12{\cdot}2) = 38 \times 10^3$ g mol^{-1} (*L. hyperborea*) the smallest (Table 4). This trend can be correlated to the predicted sol fraction versus total chain length (Fig. 8 in Stokke *et al.*, 1991). The predicted sol fraction decreases with increasing chain length qualitatively analogous to the observed shift of the molecular weight distribution of the material leached compared to the original one (Fig. 2). Figure 6 shows the correlation between $M_{90\%}$ of the experimentally determined sol fraction of the Ca-gels and the 10% percentile in the predicted sol fraction, $DP_{10\%}$, using LG_{min} as a variable parameter. Ideally, the correlation should yield a straight line with a slope equal to one on this loglog plot at the optimal LG_{min}. The data indicate that $LG_{min} = 6$ meets this criteria better than larger values of LG_{min}. Smaller values of LG_{min} were considered to be inconsistent with the calculated G-block distribution in the sol fraction of the Ca-gels (Fig. 5(B)) and were therefore not tested. The deviation from a slope of one can possibly be explained by the applicability of the second order Markov model to the whole alginate samples (see below).

Figure 7 shows a comparison of the experimentally

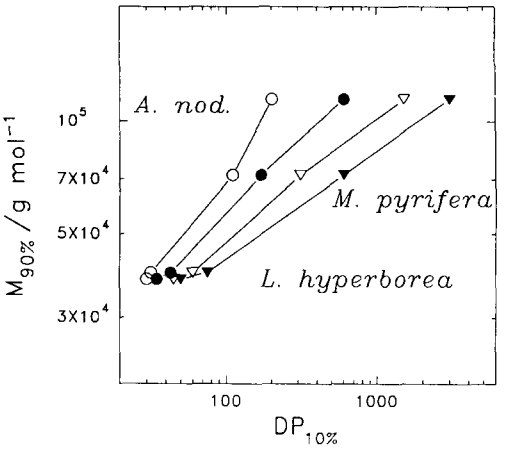

Fig. 6. Correlation between the 90% percentiles in accumulated molecular weight distribution of the experimentally determined sol fraction of Ca-alginate gel beads, $M_{90\%}$ (Table 4), and the 10% percentile in predicted sol fraction of the same sources at LG_{min} = (○) 6, (●) 8, (▽) 10 and (▼) 12.

determined and predicted chemical compositions of the sol fractions for alginates from *M. pyrifera* (lanes 1–5) and *L. hyperborea* (lanes 6–10). The predictions are shown for $LG_{min} = 4$ and 10, and degrees of polymerisation selected within the experimentally determined molecular weight distribution of the sol fractions. Major trends in the correlation between the predicted and the experimental data are as follows. The depletion in G, GG and GGG and enrichment in M, and MM are predicted to be less than observed, but the changes relative to the starting material are in the right direction. The deviations between the predictions and experiments also appear to be larger for the mannuronic acid part than the guluronic acid part. These correlation also suggest that LG_{min} should be closer to 4 than 8 ± 2 for the Ca-induced gelation.

Classical gel theories also predict a sol fraction of functional chains not associated with the polymeric network exists beyond the sol-gel transition. Because the chemical composition of such a sol fraction ideally is identical to the average chemical composition of the material, this would lead to smaller differences in

Table 4. Weight averages of starting material and sol fraction from Ca-alginate gels (T = 24°C)

Source	Starting material (10^3 g mol^{-1})			Ca-gel leaching (10^3 g mol^{-1})			
	M_n	M_w	I_p[a]	M_n	M_w	$M_{90\%}$[b]	I_p[a]
A. nodosum	107	201	1·9	49	64	115	1·31
M. pyrifera low η	75	153	2·0	39	50		1·28
M. pyrifera medium η	106	242	2·3	40	48	72	1·20
L. hyperborea PT 180	96	205	2·1	25	27	39	1·1
L. hyperborea PT 28	62	122	2·0	23	25	38	1·1

[a] $I_p = M_w/M_n$ is a polydispersity index.
[b] $M_{90\%}$ is the 90% percentile of the accumulated molecular weight distribution.

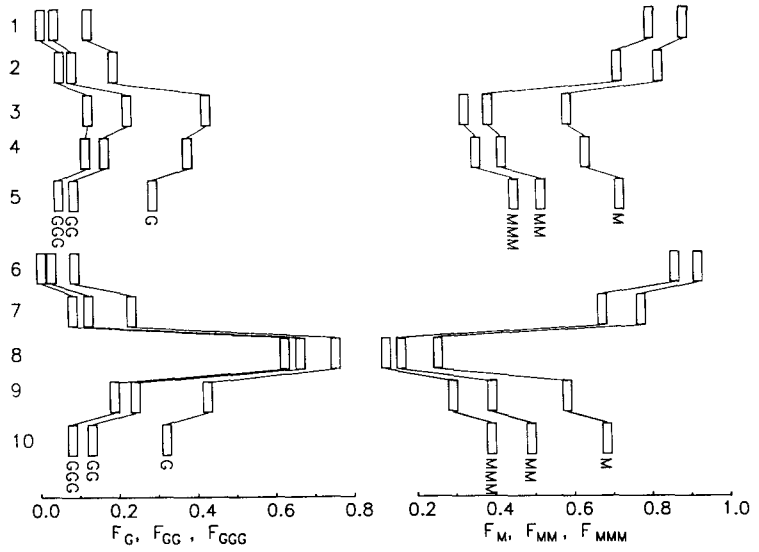

Fig. 7. Comparison of M and G content, doublets and triplets for alginate from *M. pyrifera* (lanes 1-5) and *L. hyperborea* PT 180 (lanes 6-10). Experimentally determined for starting material (3 and 8), experimentally determined for sol fraction of Ca-gels (2 and 7) and Sr-gels (1 and 6), and predicted for sol fraction at LG_{min} = 10 (4 and 9) and 4 (5 and 10).

chemical composition between the sol fraction and starting material then implied by the preceding argument. The model predictions of chemical composition of the sol fraction deviate from the observed ones by predicting less changes than observed. Inclusion of a fraction of functional chains as in classical gelation theories would thus increase the deviation between the experiments and the theory. The above-described deviation between the experimentally determined and predicted chemical composition of the sol fractions indicate that the compositional distributions are broader than that corresponding to the second-order Markov model. This is not unexpected since it is known that the average composition of alginate may vary from plant to plant, and from one type of tissue to another. Alginate samples are therefore probably mixtures of several sub-populations and even if the biosynthesis would yield second-order Markov chains, the mixtures would yield larger compositional heterogeneities. The present experimental data should therefore stimulate further investigations of the G/M distribution in alginates. Despite potential shortcomings of the second-order Markov model, this model is the simplest one that can account for the observed triad frequencies, and refinements of the sequential model will represent introduction of additional adjustable parameters.

The requirement that contiguous functional sites must exceed a critical number for formation of junction zones is not limited to alginate. The egg-box model is also the current accepted model for dimerisation of galacturonic acid blocks during gelation of pectin (Grant *et al.*, 1973; Durand *et al.*, 1990). Powell *et al.* (1982) have reported that at least 14 contiguous non-esterified galacturonic acid residues was needed to form a stable dimeric junction zone in the presence of Ca^{2+}. Iliopoulos and Audebert (1988) have likewise modelled gelation of polyacid - polybase by considering the length of non-ionised contiguous sites on the polyacid in interaction with the polybase. They assumed that the length of the neutral groups must exceed a critical value, and estimated this length by fitting the model to experimental data. Unlike these ionisable polymers where the distribution of neutral groups is a dynamic equilibrium, the alginate chains have a 'static' chemical composition allowing experimental determination of the sol fraction and thereby directly obtain information about such models. In this respect, gelation studies like the one presented here, represent a new approach to probing effects of finite chains lengths on cooperative dimerisation.

ACKNOWLEDGEMENTS

This work was partly supported by grants from the Royal Norwegian Council for Industrial and Scientific Research and from Protan Biopolymers A/S.

REFERENCES

Cesaro, A., Delben, F. & Paoletti, S. (1982). In *Thermal analysis* (Vol. II), ed. B. Miller. John Wiley & Sons: Chichester, UK, pp. 815-21.

Dubois, M., Gilles, K.A., Hamillton, J.K., Rebers, P.A. & Smith, F. (1956). *Anal. Chem.*, **28**, 350-6.

Durand, D., Bertrand, C., Busnel, J.-P., Emery, J.R., Axelos, M.A.V., Thibault, J.F., Lefebvre, J., Doublier, J.L., Clark, A.H. & Lips, A. (1990). In *Physical Networks. Polymers and Gels*, eds W. Burchard & S.B. Ross-Murphy. Elsevier Applied Science, London, UK, pp. 283-300.

Grant, G.T., Morris, E.R., Rees, D.A., Smith, P.J.C. & Thom, D. (1973). *FEBS Letts*, **32**, 195-8.

Grasdalen, H. (1983). *Carbohydr. Res.*, **118,** 255–60.
Grasdlen, H., Larsen, B. & Smidsrød, O. (1981). *Carbohydr. Res.*, **89,** 179–91.
Haug, A. & Smidsrød, O. (1970). *Acta Chem. Scand.*, **24,** 843–54.
Iliopoulos, I. & Audebert, R. (1988). *J. Polym. Sci., Polym. Phys. Ed.*, **26,** 2093–112.
Martinsen, A., Skjåk-Bræk, G. & Smidsrød, O. (1989). *Biotechnol. Bioengng.* **33,** 79–89.
Martinsen, A., Smidsrød, O., Skjåk-Bræk, G., Zanetti, Z. & Paoletti, S. (1991). *Carbohydr. Polym.*, **15,** 171–93.
Powell, D.A., Morris, E.R., Gidley, M.J. & Rees, D.A. (1982). *J. Mol. Biol.*, **155,** 517–31.
Smidsrød, O. & Skjåk-Bræk, G. (1990). *Trends Biotechnol.*, **8,** 71–8.
Soon-Shiong, P., Feldman, E., Nelson, R., Komtebedde, J., Smidsrød, O., Skjåk-Bræk, G., Espevik, T., Heintz, R. & Lee, M. (1992). *Transplantation,* **54,** 769–74.
Stokke, B.T., Smidsrød, O., Bruheim, P. & Skjåk-Bræk, G. (1991). *Macromolecules,* **24,** 4637–45.
Thom, D., Grant, G.T., Morris, E.R. & Rees, D.A. (1982). *Carbohydr. Res.*, **100,** 29–42.